Characterization and assessment of B_2O_3 added LF Slag

Suguna Soumya Varanasi[1*], Kakara Sripushpa[2], Mandalika Bhaskara Venkata Rao[3], Shaik Mahboob Basha[4], Ashok Kamaraj[5]

[1]Sr.Manager (R&D), Rashtriya Ispat Nigam Limited, Visakhapatnam Steel Plant, Visakhapatnam, India, 530031; Ph.D. student, Department of Materials Science and Metallurgical Engineering, IIT-Hyderabad, India 502285, ms22resch14005@iith.ac.in

[2]Ph.D student, Department of Materials Science and Metallurgical Engineering, IIT Hyderabad, India 502285, ms23resch02001@iith.ac.in

[3]General Manager, Corporate office, Rashtriya Ispat Nigam Limited, Visakhapatnam Steel Plant, Visakhapatnam, India, 530031, mbvenkatarao@vizagsteel.com

[4]Ph.D student, Department of Materials Science and Metallurgical Engineering, IIT Hyderabad, India 502285, ms22resch14003@iith.ac.in

[5]Assistant Professor, Department of Materials Science and Metallurgical Engineering, IIT Hyderabad, India 502285, ashokk@msme.iith.ac.in

Correspondence: ms22resch14005@iith.ac.in

Orcid: https://orcid.org/0000-0003-4502-026X

Keywords: Ladle furnace, Steelmaking, LF Slag, B_2O_3 added slag, slag valorisation, viscosity, sulphide capacity, melting temperature

ABSTRACT:

The properties of top slags play a very important role in secondary steel making. Fluxes should be chosen based on the ladle furnace (LF) slag requirements like viscosity, melting temperature, sulfide capacity, etc. CaF_2 and CaO-Al_2O_3-based synthetic slags are the most used fluxes in secondary steelmaking to improve slag fluidity and interfacial chemical reactions. CaF_2 is obsolete due to fluorine pollution and CaO-Al_2O_3 based slags have 40-50 wt % Al_2O_3 and 30-40 % CaO which is not beneficial for desulphurisation. Yet another drawback is that LF slag disintegrates into fine powder during cooling due to phase transformation C_2S ($2CaO.SiO_2$). Hence, there is a need for the development of low melting fluxes with high CaO content and the capability to prevent slag disintegration. The current work studied the effect of 0-9 wt% B_2O_3 on physico-chemical properties and characterization of LF slags. XRD analyses were carried out to identify mineralogical phases present in slag and FT-IR analysis was done to understand the changes in bonds of B_2O_3 added LF slag. The characteristic temperature of slag was determined by a hemispherical method using high-temperature microscopy. Empirical models were used to calculate viscosity, break temperature, and sulfide capacity. Factsage simulations were carried out to find the equilibrium phase fractions and percentage of liquid slag at different temperatures. New phases such as $Ca_{11}B_2Si_4O_{22}$ and $Ca_2B_3O_5$ were formed in LF slag with B_2O_3 addition. Based on the results, 0.5- 1.0 wt% B_2O_3 was found to be sufficient to prevent C_2S-driven disintegration of LF slag. Also, the Melting temperature and viscosity of LF slag were reduced by adding 3-8 wt% B_2O_3 due to the formation of BO_3 planar triangular structure and low melting eutectics in slag. Liquid slag started forming at a temperature as low as 800 ^{O}C when B_2O_3 is >6 wt%. It was found that the sulfide capacity, viscosity, and break temperature of the slag decreased with increasing wt% B_2O_3. Based on the analysis carried out, B_2O_3 can be a promising fluxing material in secondary steel making, for improving the desulphurization kinetics and valorisation potential of LF slag.

INTRODUCTION

Fluxes are important in the secondary steelmaking process, particularly in Ladle Furnace (LF) refining (Varanasi et al., 2019a). Conventional ladle fluxes are either CaF_2 or CaO-Al_2O_3 based which ensure optimum fluidity, viscosity, sulfide capacity, Liquidus temperature, thermal & and electrical conductivity, etc. (Varanasi et al., 2019b). However, the emission of fluorine causes corrosion to the equipment, environmental pollution, and health hazards (Yan et al., 2016). Even though CaO-Al_2O_3 based synthetic slags are good alternatives to CaF_2, the optical basicity of CaO-Al_2O_3 based synthetic slags is low and increased Al_2O_3 content in LF slag is not beneficial for desulfurization, deoxidation, and absorption of impurities. So, the content of Al_2O_3 in refining flux should be controlled (Wang et al., 2011a). Another problem with LF slags is, that they crumble into fine powder during cooling, due to the volume expansion associated with phase transformation of $2CaO.SiO_2$ phase (Gollapalli et al., 2020). Even though LF slag has 50-60 wt% CaO and 15-30 wt% Al_2O_3 as major constituents, its valorisation potential is low due to the disintegrating phenomena (Varanasi et al., 2022). There is a requirement for alternative fluxes, which help achieve optimum slag properties and prevent the disintegration of LF slag.

B_2O_3 is considered a promising fluxing material as an alternative to CaF_2 and CaO-Al_2O_3 based synthetic slags. It was reported by (Babenko et al., 2017) and (Wang et al., 2011c)that B_2O_3 reduces the melting point and viscosity of CaO-Al_2O_3-SiO_2-MgO based slags and for CaO–based refining flux, the fluxing action of B_2O_3 is better than that of Al_2O_3 and CaF_2. The viscosity of (composition %) 53–62 CaO, 7.5–12 SiO_2, 15–28 Al_2O_3, 8 MgO, 4 B_2O_3 slags did not exceed 0.8 Pa.s at 1500-1600^{O}C range and are very much suitable for steel desulphurization. Even though B_2O_3 is an acidic oxide and network former, it simplifies the complex silicate structure by forming BO_3^{3-} planar triangular structure (Bi et al., 2021). It was reported by (Pontikes et al., 2010) that the addition of B_2O_3 prevents the β-Ca_2SiO_4 to γ-Ca_2SiO_4 transformation in slags due to the replacement of SiO_4^{4-} units by BO_3^{3-} units. However, B_2O_3 can also form BO_4^{5-} tetrahedral structure and lead to complex structures in slag. (Wang et al., 2010a) reported that B_2O_3 may react with CaO present in slag to form low melting point eutectics such as CaO.2B_2O_3, CaO.B_2O_3, 2CaO.B_2O_3 with melting points 986^{O}C, 1154^{O}C, 1298^{O}C respectively. (Bi et al., 2021) reported that $[SiO_4]^{4-}$-$[BO_3]^{3-}$structures are formed due to addition of B_2O_3 and polymerization degree of the system will decrease. In addition, $[BO_3]^{3-}$ is a planar triangular structure that is unstable as the bond energy of B-O (787 kJ/ mol) is much larger than that of Si-O (600 kJ/mol) and Al-O (485 kJ/ mol). (Wang et al., 2012) reported that B_2O_3 has significant fluxing effect on CaO-(2CaO·SiO_2)-B_2O_3 slag system. When the content of B_2O_3 is more than 5%, the melting temperature of 2CaO·SiO_2-B_2O_3 system is lower than 1300˚C. CaO-B_2O_3 slags were used by (Wang et al., 2007) to prevent sticking of slag to the snorkel refractory. They reported that the viscosity of CaO (26-42 wt%) -Al_2O_3(40-65 Wt%)-SiO_2 (9-15 wt%) based slag decreased from 6.5 Pa.s to <2 Pa.s at 1500^{O}C. Also, the melting temperature of the slag decreased by 100^{O}C with the addition of 10 wt% CaO-B_2O_3 (mass ratio 1:1) to the slag. The addition of B_2O_3 helps in improving slag metal reaction kinetics and hence desulphurization efficiency. A highly basic slag with a low melting temperature can be achieved by the addition of B_2O_3 to the LF slag system. It was reported elsewhere (Wang et al., 2011d) (Wang et al., 2011b, 2010b) that, just by 4%B_2O_3 addition in the high basicity (5.75~7.75) CaO-based refining flux, melting temperature as low as 1250˚C can be achieved. From studies conducted by (Zhuchkov et al., 2019) there is a possibility of boron microalloying using B_2O_3 based slags. Boron can be reduced from B_2O_3 present in slag by Al or Si present in steel. (Zhang et al., 2019) reported that the addition of B_2O_3 to CaO-SiO_2 based slags increased the electrical conductivity due to the formation of BO_3^{3-} and BO_4^{5-} units whose effect is stronger than the increase in degree of polymerization caused by B_2O_3. (Babenko et al., 2019) reported that for slags with basicity (CaO/SiO_2) 4-5, the MgO saturation concentration was <7 % for 4 wt% B_2O_3. Hence, by using B_2O_3 as a fluxing agent, there is a possibility to develop a slag system with ultra-high basicity (>5), ultra-low alumina content as well as low melting temperature and low viscosity.

However, the structure-property correlation of B_2O_3 modified LF slags was not reported clearly. In the present study, an attempt was made to study the effect of B_2O_3 additions on CaO-MgO-SiO_2-Al_2O_3 based LF slag for slag stabilization and properties of slag. High-end characterization techniques such as FTIR, SEM, XRD, and high-temperature microscopy were used to study the effect of B_2O_3 addition on CaO-MgO-SiO_2-Al_2O_3 based LF slag collected from an integrated steel plant. Empirical models were used for calculating sulfide capacity, viscosity, and break temperature. Thermodynamic calculations were performed using Factsage 8.2 to estimate equilibrium phases of slag.

MATERIALS AND METHODS

Melting Experiments

LF slag was collected from an integrated steel plant and laboratory grade boric acid (H_3BO_3) with min purity of 95% is used as the source of B_2O_3. The composition of raw materials is given in Table 1.

Table 1: Chemical composition of raw materials.

Material/wt%	**CaO**	**MgO**	**SiO_2**	**Al_2O_3**	**FeO**	**MnO**	**B_2O_3**
LF slag	55	10.3	17.12	9.97	1.55	1	-
H_3BO_3	-	-	-	-	-	-	56

B_2O_3 was added in 0.25,0.5,1, 2, 3,4,6,8 wt % in LF slag and mixed thoroughly. The samples each weighing 100 gm were put into a graphite crucible and loaded in a muffle furnace with a capacity of 1700^{O}C. The slags were melted at 1600°C with a heating rate of 5 °C/min for 30 minutes. After heating, the crucible was removed, and air-cooled at room temperature as shown in Figure 1.

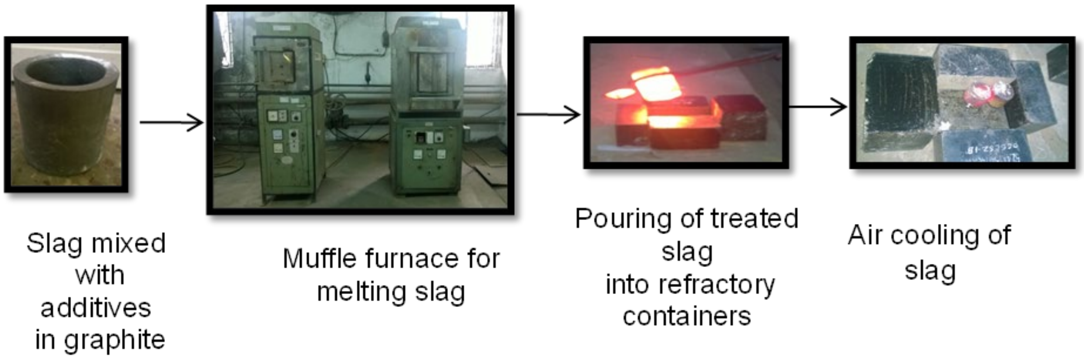

Slag mixed with additives in graphite

Muffle furnace for melting slag

Pouring of treated slag into refractory containers

Air cooling of slag

Figure 1: Schematic of slag melting experiments carried out in a muffle furnace.

Spectroscopy Analysis

Elemental chemical analysis was done for slag before and after stabilization using Panalytical axios WDXRF. Particle size analysis of LF slag was carried out using ROTAP sieve shaker. XRD analysis was carried out in Rigaku ultima IV with 2θ between 10 -90 ^{O}, Cu Kα radiation with a wavelength of 1.54A and step size of 0.02. High-temperature microscopy was used to measure the melting temperature of slag. The hemisphere method was followed to estimate slag melting temperature. Ash fusion equipment with a heating rate of 8°C/ min was used to analyse slag melting properties and the hemispherical temperature was considered as a base for comparison. FT–IR was carried out to study molecular vibrations and rotation related to covalent bonds. FTIR spectra were recorded in the wavenumber range of 600 to 1600 cm ^{1}.

Thermodynamic calculation

The effect of B_2O_3 addition on crystallization phase fractions formed in the slag and melting temperature was studied by thermodynamic software Factsage 8.2. The composition of the slag considered is given in Table 2. At constant basicity i.e 2.9, equal amounts of Al_2O_3 is replaced by B_2O_3 for analysis.

Table 2: Composition of slags considered for thermodynamic calculation.

CaO	**MgO**	**SiO_2**	**Al_2O_3**	**B_2O_3**	Basicity
56	12	19	13	0	2.9
56	12	19	12.5	0.5	2.9
56	12	19	12	1	2.9
56	12	19	10	3	2.9
56	12	19	7	6	2.9
56	12	19	4	9	2.9

RESULTS

Particle Size Analysis

200 gm of LF slag is taken, and sieving is done for 20 min using ROTAP sieve shaker. Weight retained on each sieve is measured, and graphs are plotted for mesh No vs. weight retained on each sieve and Mesh No vs. Cumulative weight as shown in Figure 2. It was found that 80% of

slag fell in the 53-106 μm size range. This fine slag as shown in Figure 3 is very difficult to recycle, store and handle. It also increases suspended particulate matter in the shop floor.

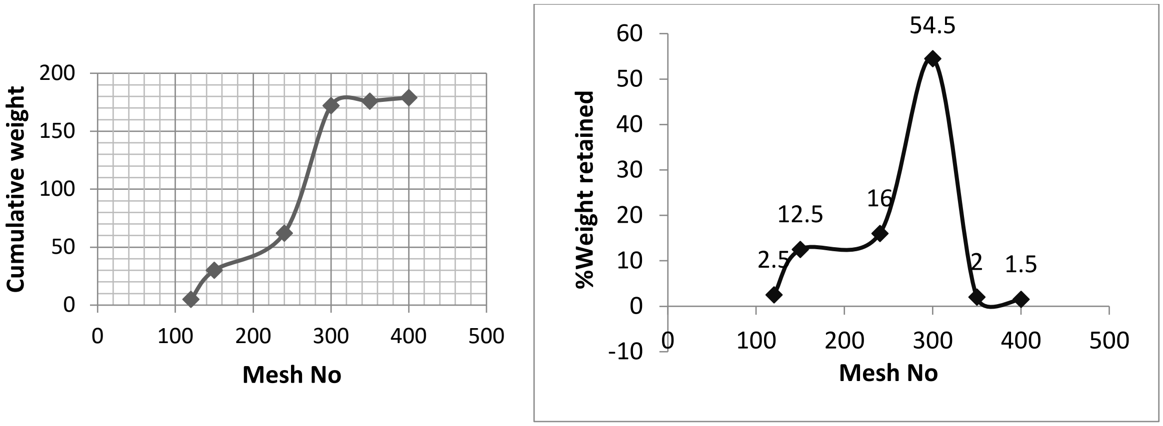

Figure 2: Sieve analysis of as received LF slag.

Figure 3:As received disintegrated LF slag.

Effect Of B_2O_3 On C_2S Stabilization

The amount of B_2O_3 in LF slag for C_2S stabilization was varied from 0.25 to 2 wt %. The treated slags are presented in Figure 4. After melting the slag, the slag was allowed to cool in the air to study the effect of B_2O_3 on the disintegration of LF slag. The figure reveals that with 0.25 wt% B_2O_3, some part of the slag disintegrated and for 100 % slag stabilization minimum of 0.5 wt% B_2O_3 addition is required. The treated slag is hard like a rock and can be used as a replacement for natural rock for road construction purposes. This process of slag stabilization is very economical as a very small quantity of borate is required and there is no need for an additional heat source to melt borates in slag. The addition of B_2O_3 can be done during steel refining or in slag pots before dumping the slag. The addition of borate sources needs to be optimized depending on slag composition and logistics in the steel industry. The compact slag generated is easier to handle and more environmentally friendly as it can be used as a partial replacement to lime and $CaO\text{-}Al_2O_3$ based synthetic slags, or else sold to the construction industry for use as a filler. However, optimization of B_2O_3 addition should be done as there is a chance of B pickup in steel from slag.

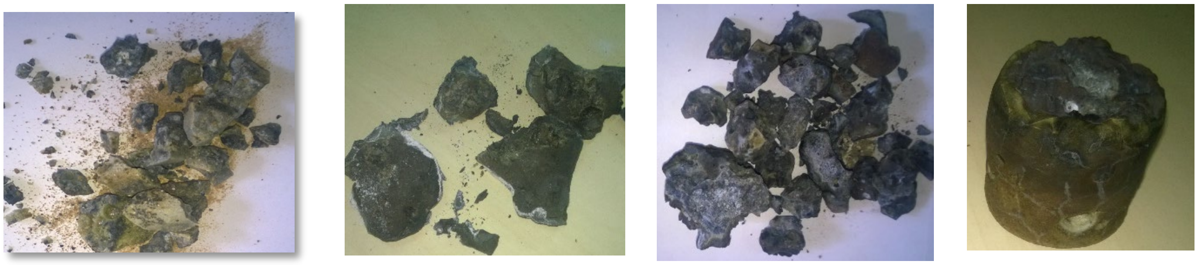

(a) 0.25 wt % B_2O_3 (b) 0.5 wt % B_2O_3 (c) 1 wt % B_2O_3 2 wt % B_2O_3

Figure 4: Visual appearance of B_2O_3 modified LF slag

Effect Of B_2O_3 On LF Slag Melting Temperature

A Slag sample of 14 mm in size was prepared in the form of a cone. It is then heated in a reducing atmosphere to analyze the melting behavior. Temperature is recorded at four points, when the rounding off of the sample tip is observed it is called deformation temperature (DT), when the height of the sample equals to width it is called softening temperature (ST), when the height of the sample is half the with it is called hemisphere temperature (HT) considered as melting temperature. And lastly, when the slag fuses and flows, it is called flow temperature (FT) as shown in Figure 5.

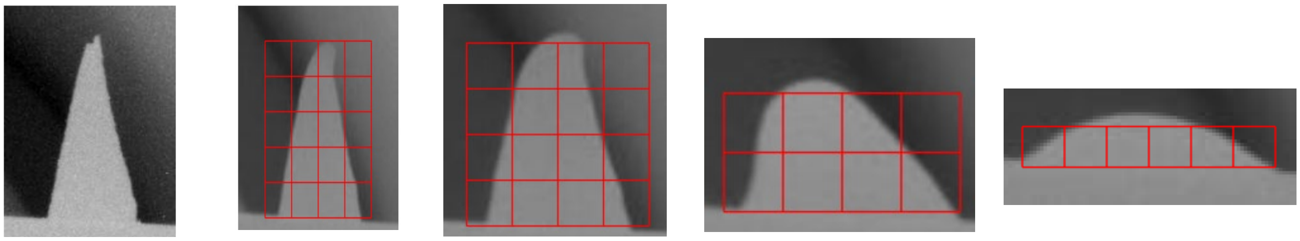

INITIAL
Temperature:815
Height: 143.25
Width: 71.65

DT
Temperature: 1400
Height: 88.02
Width: 72.00

ST
Temperature:1410
Height: 73.67
Width: 72.00

HT
Temperature: 1430
Height: 37.79
Width: 72.00

FT
Temperature: 1450
Height: 13.33
Width: 72.00

Figure 5: High temperature microscopy for estimating Slag melting temperature.

From lab scale experiments, we found that with 3-8 wt% B_2O_3 addition, the melting temperature of slag reduced from 1400 to 1110 °C as shown in Figure 6. This may be due to the formation of low melting point eutectics such as $CaO.B_2O_3$, $MgO.B_2O_3$, $CaO.2B_2O_3$, etc. When the content of B_2O_3 is 3 wt% the melting temperature is reduced from 1380 to 1300^{O}C. When the content of

B_2O_3 is from 3-6 wt% there is a gradual decrease in melting temperature from 1270 to 1225 ^{O}C. When the content of B_2O_3 is 6 wt% the slag melting temperature is 1225^{O}C. When the content of B_2O_3 exceeds 6 wt%, the temperature is reduced drastically to 1110^{O}C. Comprehensively considering the fluxing effect and cost economics, 3-4 wt% B_2O_3 is sufficient to induce the slag fluxing effect. As a result, the melting speed of lime can be improved, which is beneficial for steel desulphurization and refining efficiency.

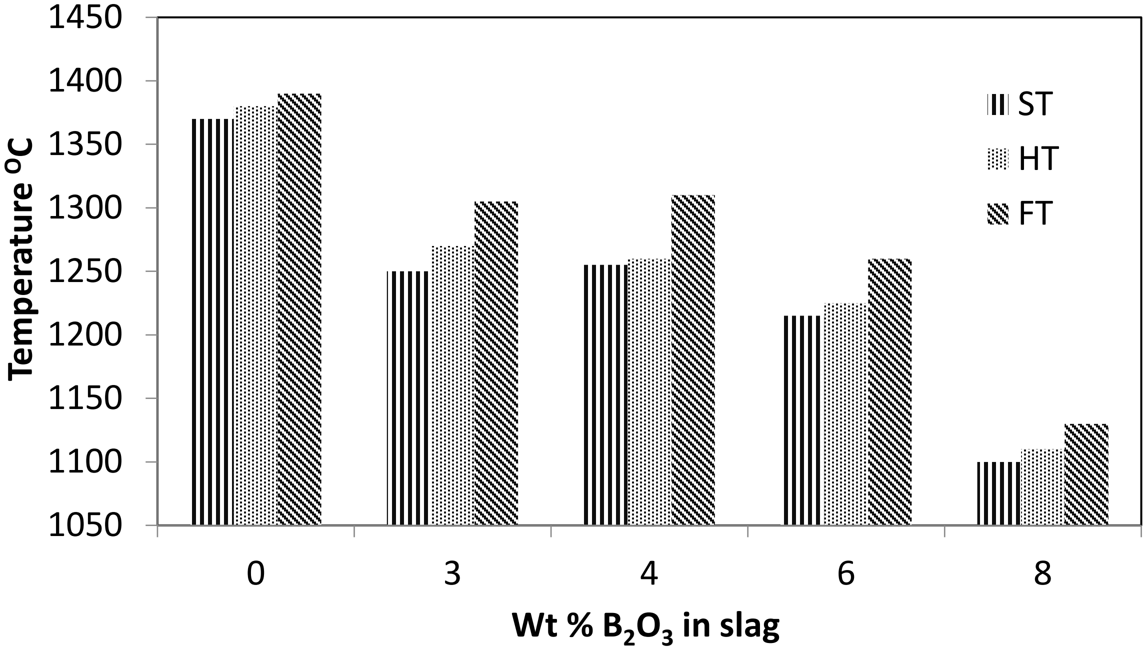

Figure 6: Effect of B_2O_3 on LF slag melting temperature from lab scale experiments.

Effect of B_2O_3 on Structural Changes in LF Slag

According to extensive studies, three basic units existed in the B_2O_3 bearing slag melts: boroxol ring, non-ring BO_3 triangular, and non-ring BO_4 tetrahedral, as shown in Figure 7. To investigate the influence of B_2O_3 addition on the structure and viscosity variation, FT–IR analysis was carried out. The results are shown in Figure 8. The FT-IR spectra curves were divided into three domains: the 600–800, 800–1200, and 1200–1600 cm^{-1} bands (Lai et al., 2020) as shown in Table 3.

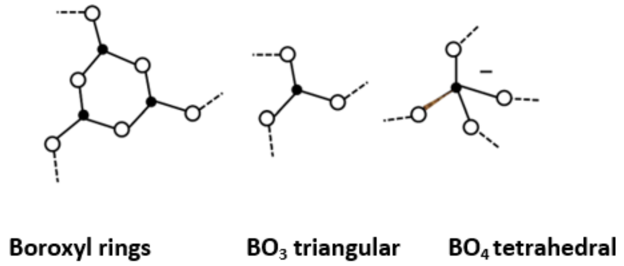

Figure 7: Basic structural units of B_2O_3 in slag melts

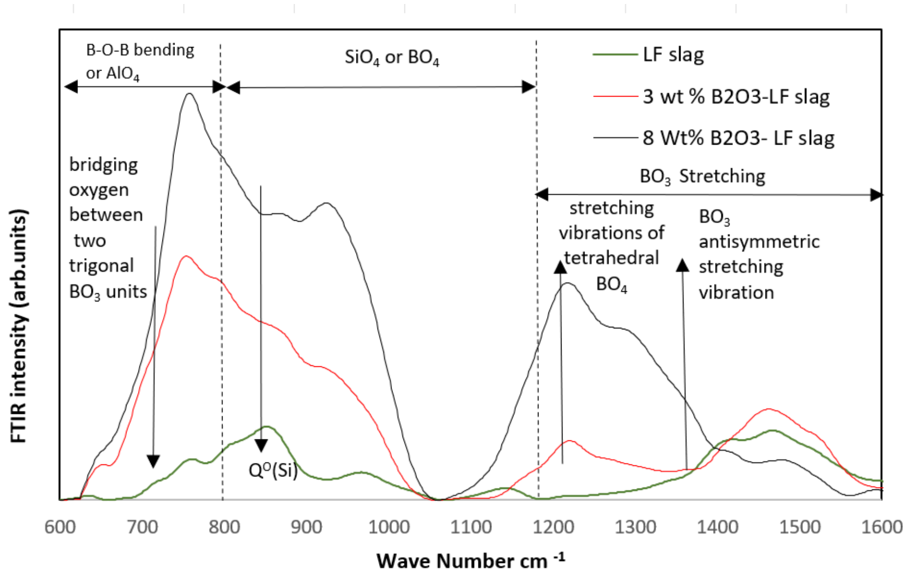

Figure 8: FT-IR spectra of B_2O_3 added CaO-MgO-SiO_2-Al_2O_3 based LF slag between 600-1600 cm^{-1}

Table 3: Assignments of FT-IR bands associated with B-O, Al-O, Si-O bonds (Sun et al., 2014) (Lai et al., 2020) (Sadaf et al., 2020) (Huang et al., 2014)

Wave number (cm^{-1})	**FTIR assignment**
600-800	bending vibrations of [AlO4] $^{5-}$ and B–O–B
800-1200	SiO_4, AlO_4, BO_4
1200-1600	BO_3 Stretching vibrations
~710	bending vibrations of bridging oxygen formed by two trigonal BO_3 units
~845	Q^0 (Si)
~1210	stretching vibrations of tetrahedral BO_4
~1350	BO_3 antisymmetric stretching vibration

The signal of the absorption region at 710 cm^{-1} became more pronounced as the B_2O_3 content increased, which indicated that BO_3 may be the main structural unit. It was observed that the intensity of the band centered at about 845 cm^{-1} gradually weakened with the increase of B_2O_3, which was assigned to Q^0(Si). The signal of trigonal BO_3 and BO_4 gradually became stronger with the increase of B_2O_3. It can be concluded that trigonal BO_3 and BO_4 were the main types of boron-related structural groups in the investigated LF slag.

Effect of B_2O_3 on LF Slag Mineralogy

The XRD of slags with different B_2O_3 from 0.5 to 8 wt% in LF slag is shown in Figure 9. The addition of B_2O_3 significantly influences the slag mineralogy. It depresses the formation of the crystalline phase and induces the formation of an amorphous glassy phase beyond 6 wt%. Similar results were reported by (Yan et al., 2014) (Priven, 2001) and consequently improves the valorisation of LF slag where glass content is important. The major phases present in LF slag are mayenite, merwinite, gehlenite, and γ-dicalcium silicate. By addition of 0.5-2 wt% B_2O_3 in LF slag disintegration was minimized and slag β-dicalcium silicate was formed due to partial replacement of SiO_4^{4-} units by BO_3^{3-} units. This replacement suppresses the Ca^{2+} migrations and SiO_4^{4-} rotations required for the β to γ transformation (Seki et al., 1986). When B_2O_3 wt% was increased from 3-8 in LF slag, phases such as $CaO.B_2O_3$, $CaO.MgO.B_2O_3$ were formed. These are low melting phases and help in decreasing the melting point of slag. Analysis of mineralogical phases is given in Table 4

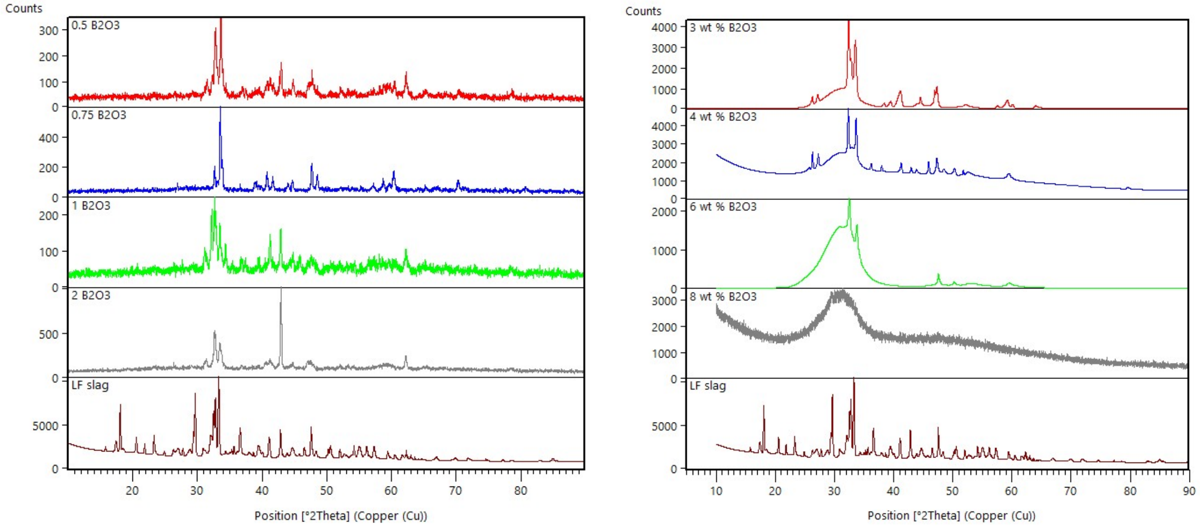

Figure 9: XRD pattern of 0.5-8 wt% B_2O_3 added CaO-MgO-SiO2-Al_2O_3 based LF slag

Table 4: Mineralogical phases present in as received LF slag and B_2O_3 added LF slag

Mineral phase	**LF slag**	**LF slag stabilized with 0.5-2 wt %B_2O_3**	**LF slag stabilized with 3-8 wt %B_2O_3**
Mayenite ($Ca_{12}Al_{14}O_{33}$)	✓	✓	✓
Merwinite ($Ca_3MgSi_2O_8$)	✓	✓	-
γ-dicalcium silicate (Ca_2SiO_4)	✓	-	-
β-dicalcium silicate (Ca_2SiO_4)	✓	✓	✓
Hatrurute (Ca_3SiO_5)	✓	✓	-
Akermanite ($Ca_2MgSi_2O_7$)	✓	✓	-
Gehlenite ($Al_2Ca_2SiO_7$)	✓	✓	-
Spinel (Mg_2SiO_4)	✓	✓	-
Periclase (MgO)	✓	-	-
Lime (CaO)	✓	-	-
calcium bisborate ($CaO.B_2O_3$)	-	-	✓
Kurchatovite ($CaO.MgO.B_2O_3$)	-	-	✓
$Ca_{11}B_2Si_4O_{22}$	-	✓	✓

Factsage analysis

From Factsage analysis it was found that the main phases in LF slag when B_2O_3 is 0 wt% are Ca_2SiO_4, Ca_3SiO_5, and Ca_3MgAlO_4. The effect of B_2O_3 on LF slag at 500 ^{O}C was studied to understand the phase changes during slag cooling as shown in *Figure 10*. With the addition of B_2O_3 a new phase, $Ca_{11}B_2Si_4O_{22}$ was found at 500^{O}C. The % of this new phase increased with B_2O_3 content from 0.5 to 6 wt% and remained constant thereafter. When B_2O_3 is >6 wt% a new phase $Ca_3B_2O_6$ is formed. With the increase in B_2O_3 from 0.5 to 3 wt%, the % of Ca_2SiO_4 decreased from 55 to 25, and with further increase of B_2O_3, Ca_2SiO_4 phase disappeared completely at 500 ^{O}C.

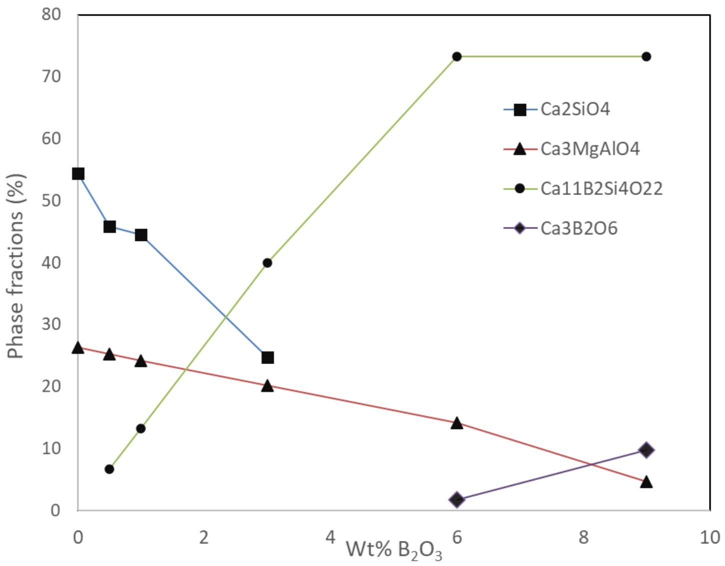

Figure 10: Effect of B_2O_3 on phase equilibria of LF slag at 500 ^{O}C

The percentage of liquid phase slag formed with B_2O_3 addition was studied as shown in Figure 11. Factsage analysis was carried out in slag with basicity of 2.9 by replacing equal amounts of Al_2O_3 with B_2O_3. When B_2O_3 is 0 wt%, the liquid phase slag started forming at 1350 ^{O}C. With the addition of B_2O_3, liquid phase slag started forming at 1100^{O}C. When 6 wt% Al_2O_3 is replaced with B_2O_3, liquid phase slag started forming at temperatures as low as 800 ^{O}C. The solidus temperature of the slag decreased with increase in wt% B_2O_3 in slag. At 1550^{O}C, around 80 % of slag is liquid when B_2O_3 is 9 wt% whereas with 0 wt% B_2O_3 only 68 % of slag is liquid. Whereas with 6 wt% B_2O_3 only 45 % of slag is liquid. Even though there is decrease in solidus temperature the % of liquid slag at steelmaking temperatures i.e at 1550 ^{O}C decreased till 6 wt% B_2O_3 and then increased at 9 wt% B_2O_3 as shown in Figure 12. This shows that different structural units are formed in slag when Al_2O_3 is replaced with B_2O_3. However, to understand the effect of B_2O_3 on slag melting temperature, further analysis needs to be carried out by varying slag basicity.

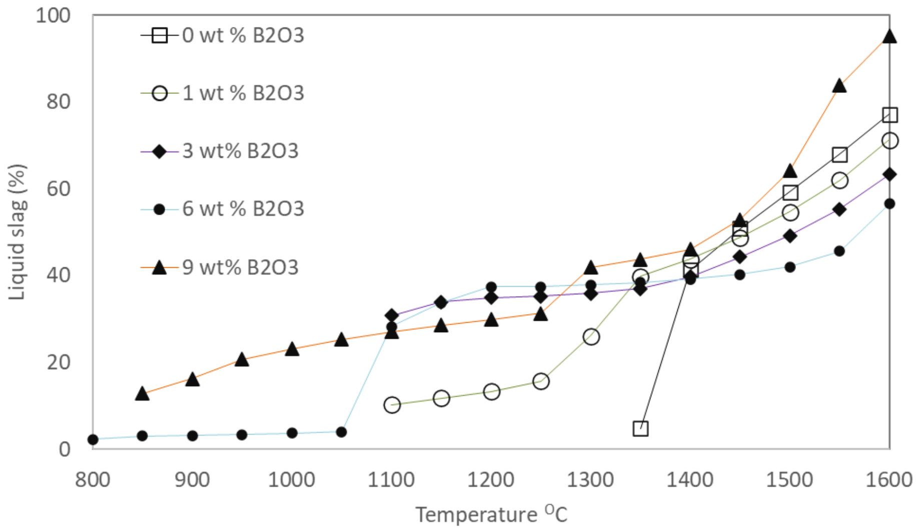

Figure 11: Effect of replacing Al_2O_3 with B_2O_3 on percentage of liquid phase slag formed at different temperatures in 56 %CaO, 12 % MgO , 19 % SiO_2, 13 % (Al_2O_3+B_2O_3)- slag wt %.

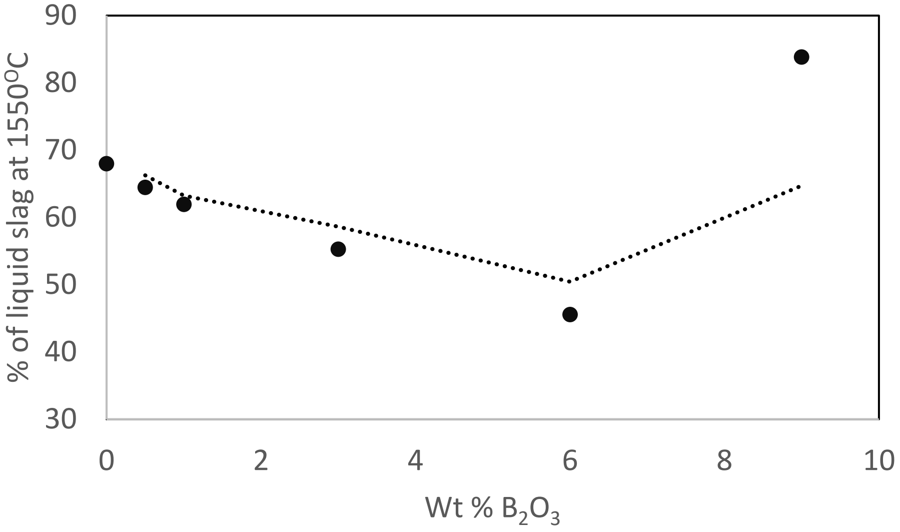

Figure 12: Effect of replacing Al_2O_3 with B_2O_3 on percentage of liquid phase slag formed at 1550°C in 56 %CaO, 12 % MgO , 19 % SiO_2, 13 % (Al_2O_3+B_2O_3) slag- wt %.

Effect Of B_2O_3 on LF Slag Viscosity, Sulphide Capacity, and Break Temperature

Several models have been developed by various researchers to estimate the sulfide capacity of slags. Earlier models were empirical and depended mainly on the optical basicity of slag and temperature. The optical basicity of various glassy and slag systems (denoted Λ) can be determined from their Pauling electronegativities. The optical basicity of a slag can be calculated from the optical basicity of individual oxides present in the slag using could be derived from equation (1) where

$$\boldsymbol{\Lambda} = \frac{\sum(\boldsymbol{X_1 n_1 \Lambda_1} + \boldsymbol{X_2 n_2 \Lambda_2} + \cdots)}{\sum(\boldsymbol{X_1 n_1} + \boldsymbol{X_2 n_2} + \cdots)} \dots\dots(\mathbf{1})$$

Table 5: Optical basicity values of individual oxides (Sosinsky and Sommerville, n.d.)

Oxide	**CaO**	**MgO**	**SiO_2**	**Al_2O_3**	**B_2O_3**
Optical basicity	1	0.78	0.48	0.61	0.42

Where Λ is the optical basicity of the slag; Λ^{th} is the optical basicity of individual oxides as shown in Table 5; as calculated from Pauling electronegativities. X is the mole fraction of individual oxides and n is the number of oxygen atoms associated with acidic and basic oxides, respectively. The sulfide capacity of B_2O_3 based LF slags was calculated from a model developed by (Sosinsky and Sommerville, n.d.) as shown in equation 2 where C_S is the sulfide capacity of the slag.

$$\log C_S = \frac{(22690-54640\Lambda)}{T} + 43.6\Lambda - 25.2\ldots(2)$$

The sulfide capacity of CaO, MgO, SiO_2, Al_2O_3, FeO, MnO (55, 11, 19, 5-14, 1,1 wt% respectively) was calculated at 1773 K by varying B_2O_3 from 0-9 wt% where an equal amount of B_2O_3 replaced with Al_2O_3. Sulfide capacity was also calculated at constant basicity by varying wt% CaO and SiO_2 (CaO/SiO_2=2.5) with MgO, Al_2O_3, FeO, MnO, B_2O_3 (10, 11, 1, 1, 0-9 wt% respectively). For both cases, it was found that the sulfide capacity of slag decreased with B_2O_3 wt% as shown in Figure 13 indicating that B_2O_3 is an acid oxide and decreases the sulfide capacity. Similar results were reported by (Yan et al., 2014).

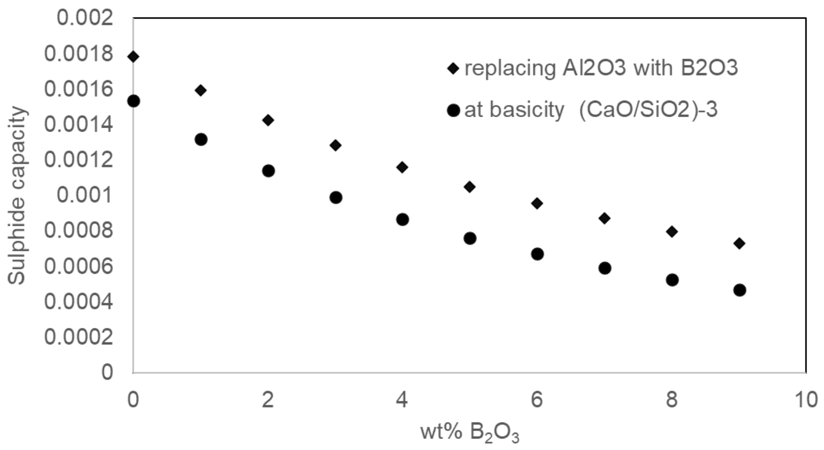

Figure 13: Effect of B_2O_3 on sulphide capacity of CaO-MgO-SiO_2-Al_2O_3-FeO-MnO based LF slags

The viscosity of slag plays an important role in kinetic conditions of steel refining particularly in desulphurization as it is slag-metal interfacial reaction.

The viscosity of molten slag depends on the internal structure of oxide melt and is affected by changes in temperature, slag composition, and oxygen partial pressure. Many models have been developed for estimating viscosities for molten oxide slag systems. For the B_2O_3 based LF slag system, the Riboud model modified by (Wang et al., 2013) was used.

$$\eta = \mathrm{AT}\exp\left(\frac{\mathrm{B}}{\mathrm{T}}\right)$$

Where ;

$\mathrm{A} = \exp[-22.47 - 2.46(\mathrm{X}_{\mathrm{CaO}} + \mathrm{X}_{\mathrm{MgO}}) + 43.07\,\mathrm{X}_{\mathrm{TiO_2}} + 72.61\mathrm{X}_{\mathrm{B_2O_3}} + 7.02(\mathrm{X}_{\mathrm{Na_2O}} + \mathrm{X}_{\mathrm{K_2O}})$-
$35.76\mathrm{X}_{\mathrm{Al_2O_3}}]$

$\mathrm{B} = 34428 - 7342(\mathrm{X}_{\mathrm{CaO}} + \mathrm{X}_{\mathrm{MgO}}) - 84121\mathrm{X}_{\mathrm{TiO_2}} - 130586\mathrm{X}_{\mathrm{B_2O_3}} - 39159(\mathrm{X}_{\mathrm{Na_2O}} +$
$\mathrm{X}_{\mathrm{K_2O}})+68833\mathrm{X}_{\mathrm{Al_2O_3}}$

T is temperature in K; η is viscosity in Pa.S.

The viscosity of CaO, MgO, SiO_2, Al_2O_3 (60, 10, 17, 4-13 wt% respectively) based slag was calculated by varying B_2O_3 from 0-9 wt%, where an equal amount of B_2O_3 is replaced with Al_2O_3. Viscosity was also calculated at constant basicity varying wt% CaO and SiO_2 (CaO/SiO_2=2.6) with MgO, Al_2O_3, B_2O_3 (10, 10, 0-9 wt% respectively). For both cases, the viscosity of slags decreased with increasing wt % B_2O_3 as shown in Figure *14*. This confirms that B_2O_3 can be used as a slag fluxing agent despite being an acidic oxide. This may be due to the formation of the BO_3 planar triangular structure. Similar results are reported by (Wang et.al.2006) (Wang et al., 2015).

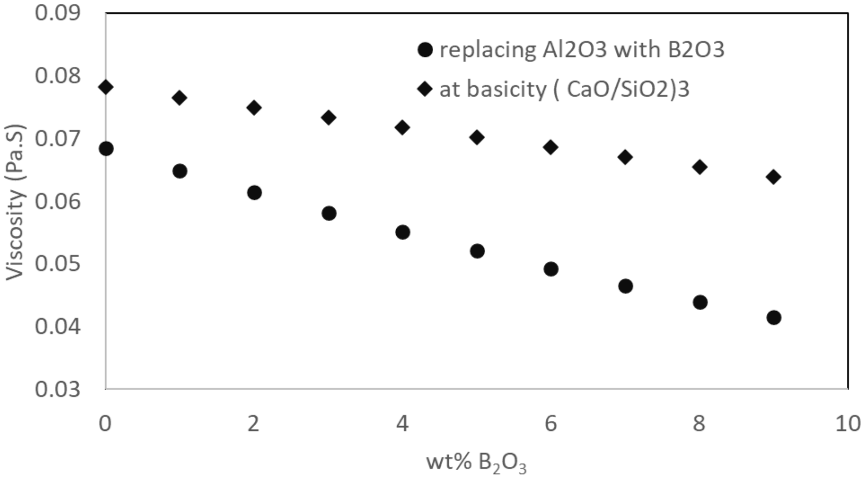

Figure 14: Effect of B_2O_3 on viscosity of CaO-MgO-SiO_2-Al_2O_3 based LF slags

The break temperature is the temperature below which there is a dramatic increase in viscosity and the slag becomes non-Newtonian in behavior. The addition of B_2O_3 plays an important role in affecting the break temperature. Break temperature (T_{br}) of the LF type slags with CaO/ SiO2 =3, Al_2O_3, B_2O_3 (15, 0-9 mol % respectively) were calculated using a model developed by (Huang et al., 2014) as shown in Equation 3 where T_{br} is in K. The break temperature reduced with an increase in B_2O_3 % as shown in Figure 15.

$$T_{br} = 1502.73 + 0.56\ \%\ CaO + 0.54\ \%\ SiO_2 - 1.41\%\ Al_2O_3 - 4.49\ \%\ Na_2O - 15.3\%\ B_2O_3 ..(3)$$

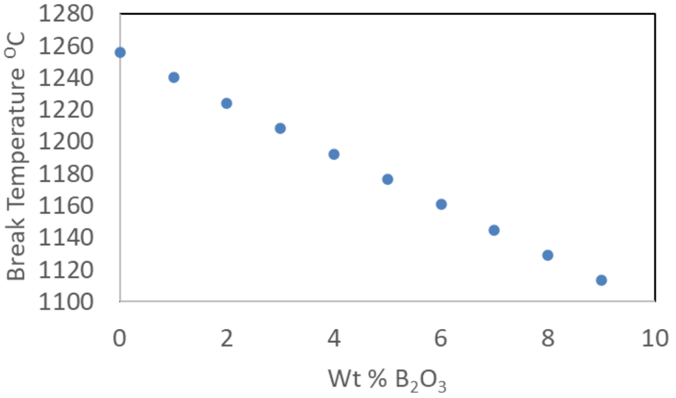

Figure 15: Effect of B_2O_3 on break temperature of CaO, SiO_2, Al_2O_3 LF slag system

CONCLUSIONS

1. From the study, it was found that B_2O_3 can act as a slag stabilizer and slag fluxing agent.
2. Around 0.5-1 wt% B_2O_3 in the studied slag system is sufficient to prevent di-calcium silicate-driven disintegration as only β-C_2S was present in B_2O_3 added LF slag. By increasing B_2O_3 wt % in LF slag, the melting point reduced from 1380 ^{O}C to 1100 ^{O}C with 8 wt % B_2O_3.
3. From XRD analysis it was found that the slag slowly transformed from crystalline to amorphous/glassy phase after 6 wt% B_2O_3 addition and melting temperature reduced drastically beyond 6 wt% B_2O_3. Low melting phases such as $CaO.B_2O_3$ and $CaO.2B_2O_3$ were also formed in investigated LF slag. Considering cost economics, and requirements in steel desulphurization 3-5 wt% B_2O_3 may be sufficient to induce a fluxing effect in LF slag.
4. FT-IR analysis also confirmed the fluxing effect of B_2O_3 as trigonal BO_3 was the main type of boron-related structural group present in the investigated LF slag. However, the effect of B_2O_3 on the properties of slag depend on CaO/SiO_2 and CaO/Al_2O_3 ratios.
5. Factsage analysis also confirmed the formation of liquid slag phases at 800 ^{O}C when B_2O_3 is >6 wt%. New phases such as $Ca_{11}B_2Si_4O_{22}$ and $Ca_2B_3O_5$ were formed in slag. At 500 ^{O}C when B_2O_3 is >3 wt%, Ca_2SiO_4 phase disappears proving that B_2O_3 helps in preventing slag disintegration. The solidus temperature of slag decreased by replacing equal amounts of Al_2O_3 with B_2O_3.
6. From empirical models, it was found that with B_2O_3 addition the sulfide capacity, viscosity, and break temperature of LF slag decreased. As desulphurization is a kinetic phenomenon compromise should be made between sulfide capacity and slag fluidity for effective interfacial chemical reactions.
7. Further studies need to be carried out to optimize B_2O_3 content for different LF slag systems considering the slag fluxing effect, sulfide capacity, and effect on basic refractory. However, B_2O_3 additions should be optimized based on slag composition and process parameters by carrying out industrial trilas.
8. There is also a need for the development of a reliable model for predicting viscosity, melting temperature, sulphide capacity, and break temperature of CaO, MgO, SiO_2, Al_2O_3, B_2O_3 based LF slag systems.

REFERENCES

Babenko, A.A., Istomin, S.A., Zhuchkov, V.I., Sychev, A. V., Ryabov, V. V., Upolovnikova, A.G., 2017. Construction of viscosity diagrams for CaO–SiO2–Al2O3–8% MgO–4% B2O3 slags by the simplex lattice method. Russian Metallurgy (Metally) 2017, 372–375. https://doi.org/10.1134/S0036029517050020

Babenko, A.A., Smetannikov, A.N., Zhuchkov, V.I., Upolovnikova, A.G., 2019. Influence of B2O3 and Basicity of CaO–SiO2–B2O3–Al2O3 Slag on the Saturation Concentration of Magnesium Oxide. Steel in Translation 49, 87–90. https://doi.org/10.3103/S0967091219020037

Bi, Z., Li, K., Jiang, C., Zhang, J., Ma, S., Sun, M., Wang, Z., Li, H., 2021. Effects of B2O3 on the structure and properties of blast furnace slag by molecular dynamics simulation. J Non Cryst Solids 551. https://doi.org/10.1016/j.jnoncrysol.2020.120412

Effect of Additives on Viscosity of LATS Refining Ladle Slag, n.d.

Gollapalli, V., Tadivaka, S.R., Borra, C.R., Varanasi, S.S., Karamched, P.S., Venkata Rao, M.B., 2020. Investigation on Stabilization of Ladle Furnace Slag with Different Additives. Journal of Sustainable Metallurgy 6, 121–131. https://doi.org/10.1007/s40831-020-00263-w

Huang, X.H., Liao, J.L., Zheng, K., Hu, H.H., Wang, F.M., Zhang, Z.T., 2014. Effect of B2O3 addition on viscosity of mould slag containing low silica content. Ironmaking and Steelmaking 41, 67–74. https://doi.org/10.1179/1743281213Y.0000000107

Lai, F., Yao, W., Li, J., 2020. Effect of B2O3on Structure of CaO-Al2O3-SiO2-TiO2-B2O3Glassy Systems. ISIJ International 60, 1596–1601. https://doi.org/10.2355/isijinternational.ISIJINT-2019-679

Pontikes, Y., Jones, P.T., Geysen, D., Blanpain, B., 2010. Options to prevent dicalcium silicate-driven disintegration of stainless steel slags. Archives of Metallurgy and Materials 55, 1167–1172. https://doi.org/10.2478/v10172-010-0020-6

Priven, A.I., 2001. Calculation of the viscosity of glass-forming melts: VI. The R2O-B2O3-SiO2 and RO-B2O3-SiO2 ternary borosilicate systems. Glass Physics and Chemistry 27, 360–370. https://doi.org/10.1023/A:1011372328059

Sadaf, S., Wu, T., Zhong, L., Liao, Z.Y., Wang, H.C., 2020. Effect of basicity on the structure, viscosity and crystallization of CaO-SiO2-b2o3 based mold fluxes. Metals (Basel) 10, 1–12. https://doi.org/10.3390/met10091240

Seki, A., Aso, Y., Okubo, M., Sudo, F., Ishizaka, K., 1986. Development of Dusting Prevention Stabilizer for Stainless Steel Slag. Kawasaki Steel Technical Report.

Sosinsky, D.J., Sommerville, I.D., n.d. The Composition and Temperature Dependence of the Sulfide Capacity of Metallurgical Slags.

Sun, Y., Liao, J., Zheng, K., Wang, X., Zhang, Z., 2014. Effect of B2O3 on the Structure and Viscous Behavior of Ti-Bearing Blast Furnace Slags. JOM 66, 2168–2175. https://doi.org/10.1007/s11837-014-1087-8

Varanasi, S.S., More, V.M.R., Rao, M.B.V., Alli, S.R., Tangudu, A.K., Santanu, D., 2019a. Recycling Ladle Furnace Slag as Flux in Steelmaking: A Review. Journal of Sustainable Metallurgy. https://doi.org/10.1007/s40831-019-00243-9

Varanasi, S.S., Pathak, R.K., Sahoo, K.K., More, V.M.R., Santanu, D., Alli, S.R., 2019b. Effect of CaO–Al2O3-Based Synthetic Slag Additions on Desulphurisation Kinetics of Ladle Furnace Refining. Transactions of the Indian Institute of Metals 72, 1447–1452. https://doi.org/10.1007/s12666-019-01616-0

Varanasi, S.S., Rao, M.V.M., Santanu, D., Alli, R., Kumar, D.S.V.S., Tangudu, A.K., Gollapalli, V., Pathak, R.K., Santhamma, C.S., 2022. Effect of recycling ladle furnace slag as flux on steel desulphurization during secondary steel making secondary steel making. Ironmaking & Steelmaking 0, 1–8. https://doi.org/10.1080/03019233.2022.2060459

Wang, H., Yang, L., Zhu, H., Yan, Y., 2011a. Comparison of effects of B2O3 and CaF2 on metallurgical properties of high basicity CaO-based flux, in: Advanced Materials Research. pp. 966–969. https://doi.org/10.4028/www.scientific.net/AMR.311-313.966

Wang, H., Yang, L., Zhu, H., Yan, Y., 2011b. Comparison of effects of B2O3 and CaF2 on metallurgical properties of high basicity CaO-based flux. Adv Mat Res 311–313, 966–969. https://doi.org/10.4028/www.scientific.net/AMR.311-313.966

Wang, H., Zhang, T., Zhu, H., Li, G., Yan, Y., Wang, J., 2011c. Effect of B 2 O 3 on Melting Temperature, Viscosity and Desulfurization Capacity of CaO-based Refining Flux, ISIJ International.

Wang, H., Zhang, T., Zhu, H., Li, G., Yan, Y., Wang, J., 2011d. Effect of B2O3 on melting temperature, viscosity and desulfurization capacity of CaO-based refining flux. ISIJ International 51, 702–706. https://doi.org/10.2355/isijinternational.51.702

Wang, H.M., Li, G.R., Dai, Q.X., Li, B., Zhang, X.J., Shi, G.M., 2007. CAS-OB refining: Slag modification with B2O3-CaO and CaF2-CaO. Ironmaking and Steelmaking 34, 350–353. https://doi.org/10.1179/174328107X155277

Wang, H.M., Li, G.R., Li, B., Zhang, X.J., Yan, Y.Q., 2010a. Effect of B2O3 on Melting Temperature of CaO-Based Ladle Refining Slag. Journal of Iron and Steel Research International 17, 18–22. https://doi.org/10.1016/S1006-706X(10)60177-X

Wang, H.M., Li, G.R., Li, B., Zhang, X.J., Yan, Y.Q., 2010b. Effect of B2O3 on Melting Temperature of CaO-Based Ladle Refining Slag. Journal of Iron and Steel Research International 17, 18–22. https://doi.org/10.1016/S1006-706X(10)60177-X

Wang, H.M., Li, P.S., Li, G.R., Zhang, M., Zhao, Z., Zhao, Y., 2012. The melting temperature of CaO-(2CaO·SiO2)-B2O3-SiO2-(Al2O3) slag system, in: Applied Mechanics and Materials. pp. 35–38. https://doi.org/10.4028/www.scientific.net/AMM.217-219.35

Wang, L., Cui, Y., Yang, J., Zhang, C., Cai, D., Zhang, J., Sasaki, Y., Ostrovski, O., 2015. Melting Properties and Viscosity of SiO2-CaO-Al2O3-B2O3 System. Steel Res Int 86, 670–677. https://doi.org/10.1002/srin.201400353

Wang, Z., Shu, Q., Chou, K., 2013. Viscosity of Fluoride-Free Mold Fluxes Containing B2O 3 and TiO2. Steel Res Int 84, 766–776. https://doi.org/10.1002/srin.201200256

Yan, P., Nie, P., Huang, S., Blanpain, B., Guo, M., 2014. Sulphide capacity and mineralogy of BaO and B2O3 modified CaO-Al2O3 top slag. ISIJ International 54, 1570–1577. https://doi.org/10.2355/isijinternational.54.1570

Yan, W., Chen, W., Yang, Y., Lippold, C., McLean, A., 2016. Evaluation of B2O3 as replacement for CaF2 in CaO–Al2O3 based mould flux. Ironmaking and Steelmaking 43, 316–323. https://doi.org/10.1179/1743281215Y.0000000062

Zhang, P., Liu, J., Wang, Z., Qian, G., Ma, W., 2019. Effect of B2O3 Addition on Electrical Conductivity and Structural Roles of CaO-SiO2-B2O3 Slag. Metallurgical and Materials Transactions B: Process Metallurgy and Materials Processing Science 50, 304–311. https://doi.org/10.1007/s11663-018-1472-8

Zhuchkov, V.I., Salina, V.A., Sychev, A. V., 2019. The Study of the Process of Metal-Thermal Reduction of Boron from the Slag of the System CaO-SiO2-MgO-Al2O3-B2O3, in: Materials Science Forum. Trans Tech Publications Ltd, pp. 423–429. https://doi.org/10.4028/www.scientific.net/MSF.946.423